

Electronic Supporting Information

## Two cases of In-MOFs with gas adsorption and separation capability based on different pyridinyl carboxylate linkers

Fei Liang<sup>acl</sup>, Jiaqi Liang<sup>a1</sup>, Dan Gao<sup>b</sup>, Lingheng Kong<sup>d</sup>, Shuo Huang<sup>c</sup>, Yayuan Guo<sup>c</sup>, Changkui Liu<sup>c\*</sup>, Tao Ding<sup>b\*</sup>

<sup>a</sup> School of Pharmacy, Xi'an Medical University, Xi'an, 710021, China

<sup>b</sup> School of Environmental and Chemical Engineering, Xi'an Polytechnic University, Xi'an, 710048 China

<sup>c</sup> Research Center of Tooth and Maxillofacial Tissue Regeneration and Restoration, School of Stomatology, Xi'an Medical University, Xi'an, Shaanxi 710021, China

<sup>d</sup> School of Basic Medicine, Xi'an Medical University, Xi'an, 710021, China

<sup>1</sup> These authors contributed equally to this work and should be considered co-first authors.

**Table S1 Selected Bond Length (Å) and Angles (°) for In-MOF 1 and In-MOF 2**

In-MOF 1			
In(3)-O(7)	2.055(7)	In(3)-O(2)#1	2.182(5)
In(3)-O(2)#2	2.182(5)	In(3)-O(1)#3	2.165(5)
In(3)-O(1)#4	2.165(5)	In(3)-O(8)	2.127(9)
In(2)-O(7)	1.987(14)	In(2)-O(3)#1	2.148(6)
In(2)-O(3)	2.148(6)	In(2)-O(3)#2	2.148(6)
In(2)-O(3)#5	2.148(6)	In(2)-O(6)	2.230(13)
In(1)-O(5)#6	2.128(6)	In(1)-O(5)#7	2.128(6)
In(1)-O(5)	2.128(6)	In(1)-O(5)#8	2.128(6)
In(1)-O(4)	2.559(7)	In(1)-O(4)#7	2.559(7)

In(1)-O(4)#8	2.559(7)	In(1)-O(4)#6	2.559(7)
O(7)-In(3)-O(2)#2	96.2(3)	O(7)-In(3)-O(2)#1	96.2(3)
O(7)-In(3)-O(1)#4	92.0(3)	O(7)-In(3)-O(1)#3	92.0(3)
O(7)-In(3)-O(8)	176.1(4)	O(2)#2-In(3)-O(2)#1	82.4(3)
O(1)#4-In(3)-O(2)#1	169.7(2)	O(1)#3-In(3)-O(2)#1	90.5(2)
O(1)#4-In(3)-O(2)#2	90.5(2)	O(1)#3-In(3)-O(2)#2	95.6(3)
O(8)-In(3)-O(2)#2	86.7(2)	O(8)-In(3)-O(2)#1	86.7(2)
O(8)-In(3)-O(1)#4	85.5(2)	O(8)-In(3)-O(1)#3	85.5(2)
O(7)-In(2)-O(3)#5	93.71(16)	O(7)-In(2)-O(3)#2	93.71(16)
O(7)-In(2)-O(3)	93.71(16)	O(7)-In(2)-O(3)#1	93.71(16)
O(7)-In(2)-O(6)	180.0	O(3)#1-In(2)-O(3)#2	87.2(3)
O(3)#5-In(2)-O(3)#2	92.4(3)	O(3)#5-In(2)-O(3)#1	172.6(3)
O(3)#1-In(2)-O(3)	87.1(3)	O(3)#2-In(2)-O(3)	172.6(3)
O(3)#1-In(2)-O(6)	86.29(16)	O(3)#5-In(2)-O(6)	86.29(16)
O(3)-In(2)-O(6)	86.29(16)	O(3)#2-In(2)-O(6)	86.29(16)
O(5)-In(1)-O(5)#8	78.9(4)	O(5)-In(1)-O(5)#6	137.4(4)
O(5)#6-In(1)-O(5)#7	78.9(4)	O(5)#6-In(1)-O(5)#8	117.1(4)
O(5)-In(1)-O(5)#7	117.2(4)	O(5)#8-In(1)-O(5)#7	137.4(4)
O(5)-In(1)-O(4)	56.1(3)	O(5)-In(1)-O(4)#7	85.3(2)
O(5)#6-In(1)-O(4)#6	56.1(3)	O(5)#6-In(1)-O(4)	89.2(3)
O(5)#7-In(1)-O(4)#7	56.1(3)	O(5)#8-In(1)-O(4)	130.8(3)
O(5)#7-In(1)-O(4)#6	130.8(3)	O(5)#7-In(1)-O(4)	85.3(2)
O(5)#6-In(1)-O(4)#7	130.8(3)	O(5)-In(1)-O(4)#8	130.8(3)
O(5)-In(1)-O(4)#6	89.2(3)	O(5)#6-In(1)-O(4)#8	85.3(2)
O(5)#8-In(1)-O(4)#6	85.3(2)	O(5)#8-In(1)-O(4)#8	56.1(3)
O(5)#7-In(1)-O(4)#8	89.2(3)	O(5)#8-In(1)-O(4)#7	89.2(3)

Symmetry code: #1 -y+3/2,-x+3/2,z; #2 -x+3/2,-y+3/2,z; #3 y+1/2,-x+1,-z+3/2; #4 -x+1/2,y+1,-z+3/2; #5 y,x,z; #6 -y+1,-x+1,-z+1; #7 -x+2/3,-y+1/2,z; #8 y+1/2,x+1/2,-z+1; #9 -y+1,x-1/2,-z+3/2.

---

## In-MOF 2

---

In(1)-O(8)#1	2.130(14)	In(1)-O(4)	2.139(15)
In(1)-O(6)	2.205(17)	In(1)-N(1)#2	2.308(19)
In(1)-O(1)	2.397(17)	In(1)-O(2)	2.40(2)
In(1)-O(5)	2.40(2)	In(1)-O(3)	2.57(2)
O(8)#1-In(1)-O(4)	146.3(8)	O(8)#1-In(1)-O(6)	100.9(6)
O(4)-In(1)-O(6)	88.9(7)	O(8)#1-In(1)-N(1)#2	89.1(6)
O(4)-In(1)-N(1)#2	124.3(7)	O(6)-In(1)-N(1)#2	82.8(6)
O(8)#1-In(1)-O(1)	93.7(6)	O(4)-In(1)-O(1)	89.1(7)
O(6)-In(1)-O(1)	156.6(6)	N(1)#2-In(1)-O(1)	79.1(6)
O(8)#1-In(1)-O(2)	79.2(7)	O(4)-In(1)-O(2)	75.5(8)
O(6)-In(1)-O(5)	56.1(7)	N(1)#2-In(1)-O(5)	134.9(7)
O(1)-In(1)-O(5)	134.9(7)	O(1)-In(1)-O(5)	145.3(7)
O(2)-In(1)-O(5)	91.5(8)	O(8)#1-In(1)-O(3)	162.6(7)
O(4)-In(1)-O(3)	50.4(7)	O(6)-In(1)-O(3)	81.0(7)
N(1)#2-In(1)-O(3)	73.9(6)	O(1)-In(1)-O(3)	79.7(7)
O(2)-In(1)-O(3)	112.4(8)		

Symmetry code: #1  $x+1/2, y-3/2, z+1/2$ ; #2  $-x+3/2, y+1/2, -z+5/2$ ; #3  $x+1/2, -y+3/2, z-1/2$ ; #4  $-x+3/2, y-1/2, -z+5/2$ ; #5  $x-1/2, -y+3/2, z+1/2$ ; #6  $x-1/2, -y+3/2, z-1/2$ .

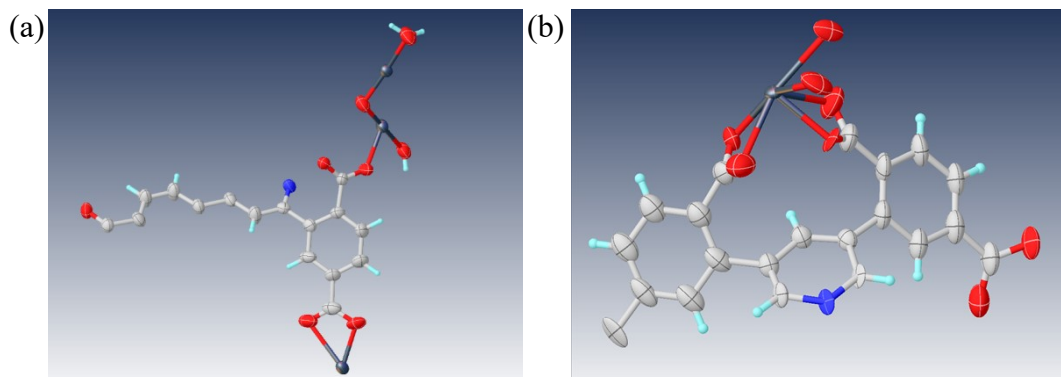


**Fig. S1** The structural drawing showing ADPs of (a) In-MOF 1 and (b) In-MOF 2.

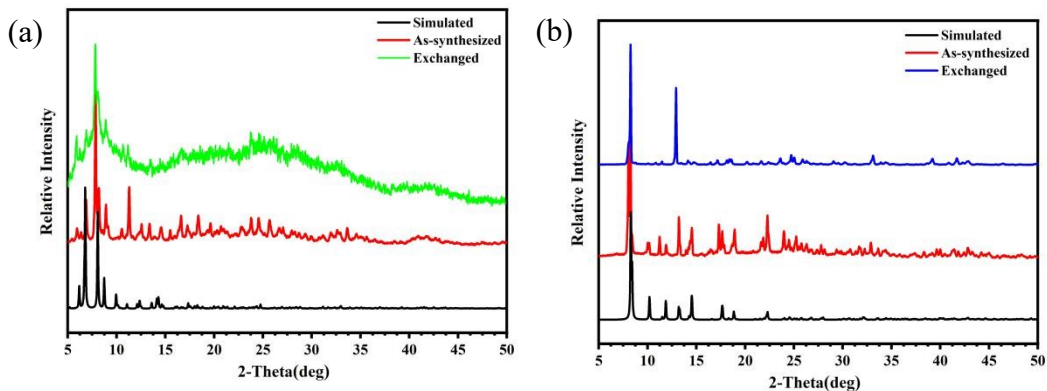


**Fig. S2** PXRD patterns for (a) In-MOF 1 and (b) In-MOF 2: Simulated, as-synthesized,solvent exchange samples.

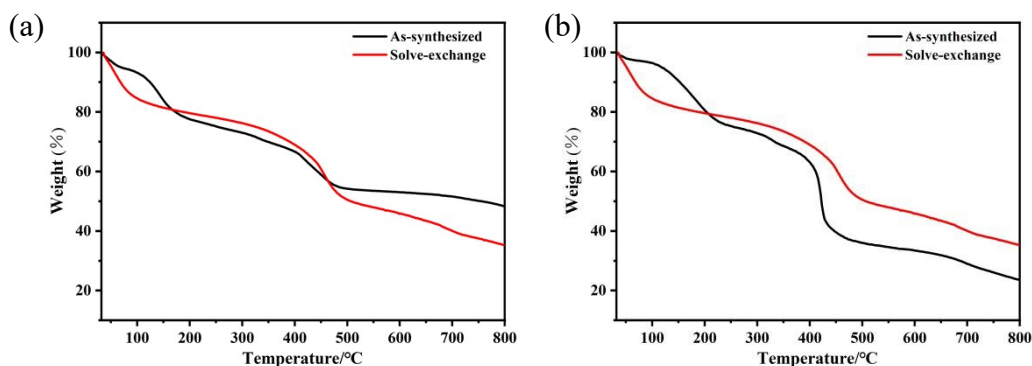


**Fig. S3** The TGA curve of (a) In-MOF 1 and (b) In-MOF 2.

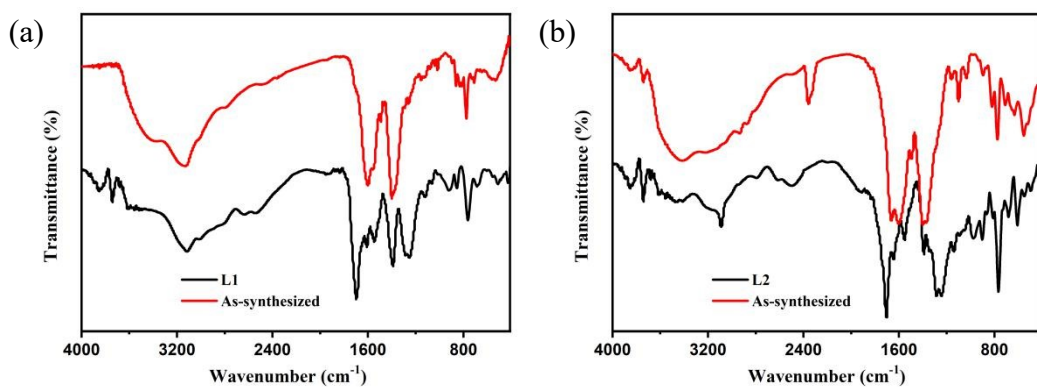


**Fig. S4** IR for (a) In-MOF 1 and (b) In-MOF 2: ligand and as-synthesized samples.

#### IAST adsorption selectivity calculation

The experimental isotherm data for pure C<sub>2</sub>H<sub>2</sub>, CO<sub>2</sub> and CH<sub>4</sub> (measured at 298 K) were fitted using a Langmuir-Freundlich (L-F) model

$$q = \frac{a * b * p^c}{1 + b * p^c}$$

Where  $q$  and  $p$  are adsorbed amounts and pressures of component  $i$ , respectively. The adsorption selectivities for binary mixtures of  $\text{C}_2\text{H}_2/\text{CH}_4$  and  $\text{CO}_2/\text{CH}_4$ , defined by

$$S_{i/j} = \frac{(x_i^* y_j)}{(x_j^* y_i)}$$

were calculated using the Ideal Adsorption Solution Theory (IAST) of Myers and Prausnitz.

Where  $x_i$  the mole fraction of component  $i$  in the adsorbed phase and  $y_i$  is the mole fraction of component  $i$  in the bulk.

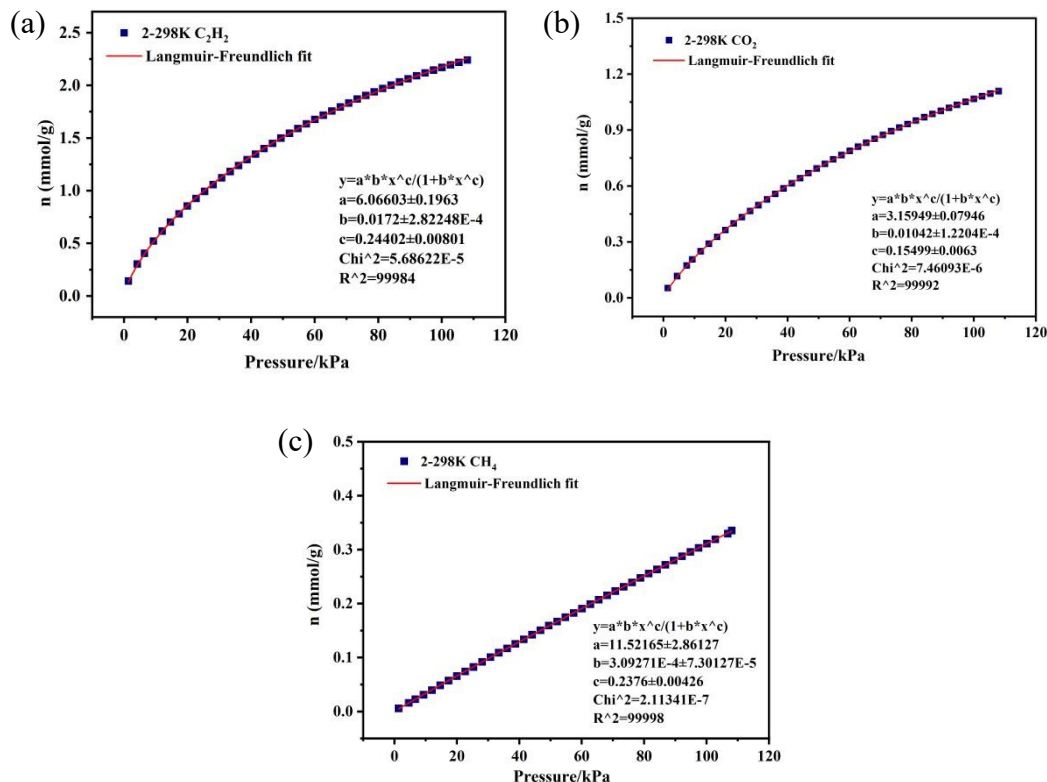


**Fig. S5** (a)  $\text{C}_2\text{H}_2$ , (b)  $\text{CO}_2$  and (c)  $\text{CH}_4$  adsorption isotherms of In-MOF 1 at 298 K with fitting by L-F model

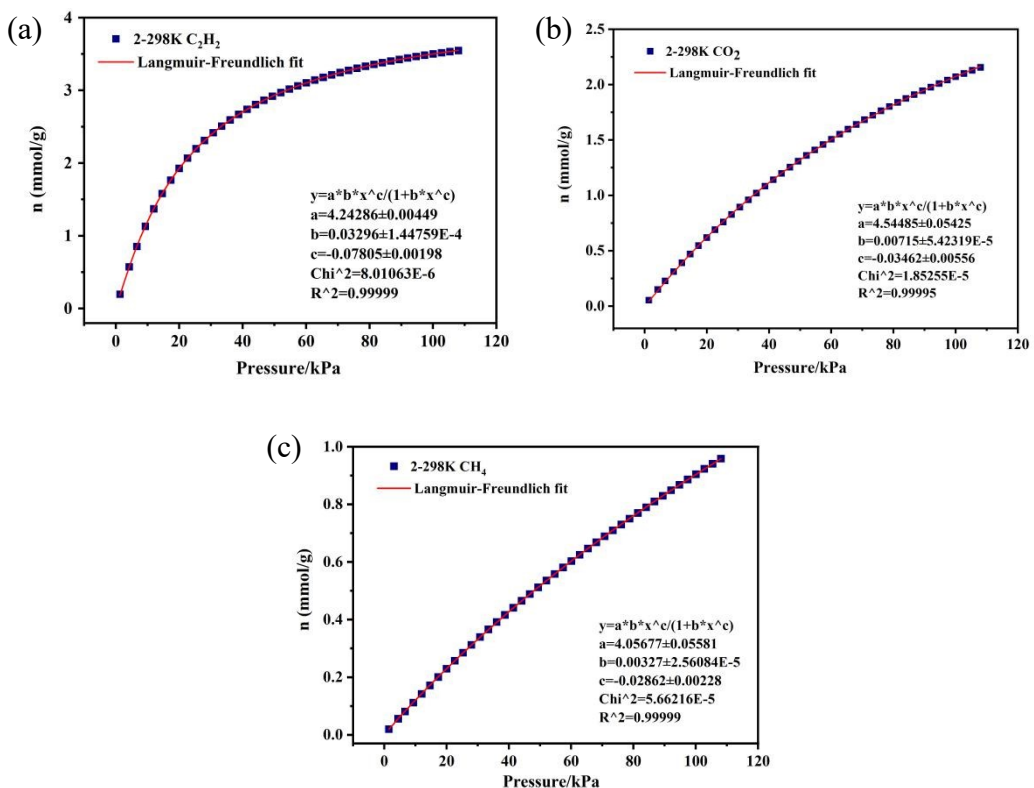


**Fig. S6** (a)  $C_2H_2$ , (b)  $CO_2$  and (c)  $CH_4$  adsorption isotherms of In-MOF 2 at 298 K with fitting by L-F model

#### Calculation of sorption heat for $C_2H_2$ and $CO_2$ uptakes using Virial 2 model

The above equation was applied to fit the combined  $C_2H_2$  and  $CO_2$  and isotherm data for desolvated **1a** at 273 and 298 K, where  $P$  is the pressure,  $N$  is the adsorbed amount,  $T$  is the temperature,  $a_i$  and  $b_i$  are virial coefficients, and  $m$  and  $n$  are the number of coefficients used to describe the isotherms.  $Q_{st}$  is the coverage-dependent enthalpy of adsorption and  $R$  is the universal gas constant.

$$\ln P = \ln N + 1/T \sum_{i=0}^m a_i N^i + \sum_{i=0}^n b_i N^i Q_{st} = -R \sum_{i=0}^m a_i N^i$$

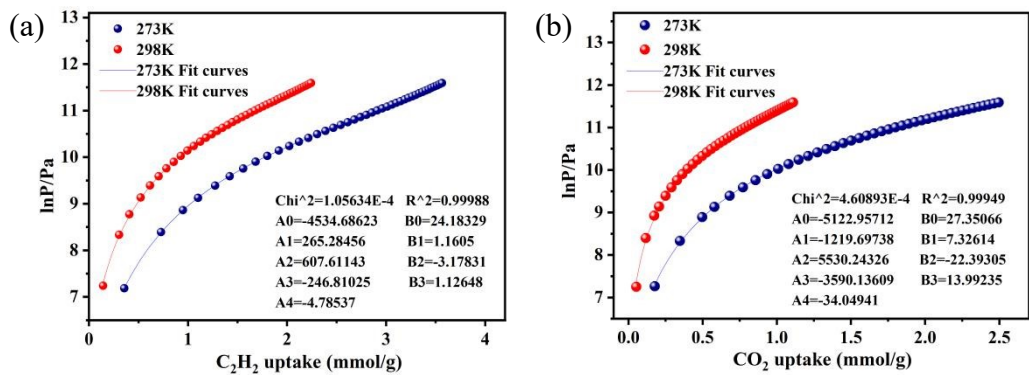


**Fig. S7** Virial analysis of the  $\text{C}_2\text{H}_2$  and  $\text{CO}_2$  adsorption data at 273 K and 298 K for In-MOF 1.

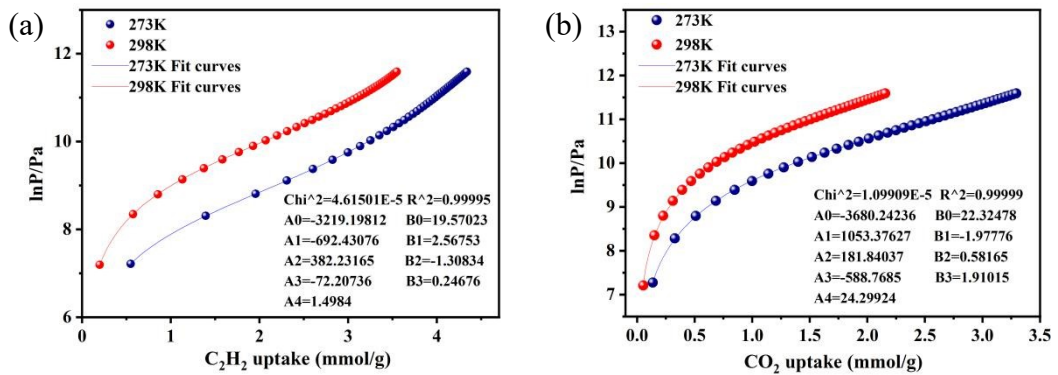


**Fig. S8** Virial analysis of the  $\text{C}_2\text{H}_2$  and  $\text{CO}_2$  adsorption data at 273 K and 298 K for In-MOF 2.